Journal of Operation and Automation in Power Engineering
Vol. 11, No. 3, Oct.. 2023, Pages: 223-229
http://joape.uma.ac.ir

# A Decentralized Energy Management Method for Load Curve Smoothing Considering Demand and Profit of Electric Vehicle Owners with Different Capacity of Batteries

*V. Bagheri*[1], *A. F. Ehyaei*[1,*], *M. Haeri*[2]

[1] *Department of Electrical Engineering, Imam Khomeini International University, Qazvin, Iran*
[2]*Department of Electrical Engineering, Sharif University of Technology, Tehran. Iran*

***Abstract-*** *Increasing requirements of electric vehicles with different capacities of batteries and increasing number of small-sized renewable energy sources lead to complexity of calculations, voltage drop, power quality loss, and unevenness in the load curve. This paper proposes a modified version of the mean-field decentralized method to smooth the load curve, maximize vehicle owners' profit, and meet vehicle owners' demands. Different capacity of batteries is a challenging problem in the charging and discharging control of electric vehicles; so to solve this problem, a weighted average method is used, which determines the design weighting parameters based on the capacity of batteries. Finally, a comparison has been made between five different centralized and decentralized strategies with weighted and weightless average methods.*

***Keyword:*** Electrical vehicle, Arrival & departure time, Initial & final SoC, Load curve, Weighted mean-field.

## 1. INTRODUCTION

Due to the small size of some distributed generation resources, such as small-sized wind turbines and photovoltaics, these resources are often installed near the consumer [1]. In this regard some approaches have been proposed to integrating small-scale distributed energy sources into low and medium-voltage networks with renewable energies [2]. In such networks, the demand-side management algorithms help to reduce the peak-to-average ratio by increasing the cost of electricity and using renewable energy resources [3]. Therefore, due to increasing energy consumption costs and also lack of resources to meet the needs, electric vehicles can be used for two-way energy exchange [4]. Using these vehicles is one of the optimal solutions to overcome the problem of fossil fuels and global warming [5]. Due to the increasing number of electric vehicles and renewable energy sources, the need to use energy management in smart grids is observed. By using energy management, the peak load could be reduced, which leads to increased network stability and reduced operating costs [6]. Because of the variable nature of renewable energy sources, energy storage devices such as batteries can help to maintain the voltage quality [7]. However, uncoordinated charging of electric vehicles leads to overload, power quality loss, and voltage fluctuations, which is very harmful to distribution networks [8]. To persuade vehicle owners to share their batteries with the smart grid, both profit and requests must be met (vehicle requirements). For this purpose, each vehicle notifies the required final state of charge (SoC) at arrival time to the aggregator. However, considering the initial and the final SoC lead to complexity of calculations and increases the time to perform calculations.

A battery charge and discharge algorithm has been proposed in [9] for managing alternating renewable sources, real-time network data for peak load shaving, power curve smoothing, and voltage regulation of a distribution transformer. A solution for high penetration of renewable energy using a battery energy storage system with the peak shaving and load curve smoothing was presented [10]. High penetration of renewable energy is considered in [9, 10], but the vehicle requirements are not considered. Control of the diesel generators and wind turbines in [11] enables the battery to smooth the wind and load changes, improve the power quality of the islanded system, adjust the frequency and reduce the peak. In [12], the load curve

Received: 01 Apr. 2022
Revised: 04 May 2022
Accepted: 18 Jun. 2022
∗Corresponding author:
E-mail: f.ehyaei@eng.ikiu.ac.ir (A. F. Ehyaei)
DOI: 10.22098/joape.2023.10583.1758
***Research Paper***

of a system consisting of diesel generators, PV farms, and batteries is smoothed in an islanded state based on load prediction, and the peak of the load curve is shaved. Also, the power system in [11, 12] is considered for islanded mode. An electric vehicle to grid energy management system presented in [13] to peak shaving, valley filling, and load balancing in a grid-connected microgrid helps to smooth the load curve and better use of microgrids. The main purpose of the system is to reduce critical customer demand, load demand, fill off-peak periods, and electricity price variation. An optimal priority-based vehicle-to-grid scheduling to minimize the grid load variance is proposed in [14] and can operate in valley filling, peak load shaving, and priority charging modes. The electric vehicle charging can be performed in all three modes, and the electric vehicle discharging only occurs during peak load shaving mode.

Two decentralized electric vehicle charge scheduling schemes for smoothing the load curve of residential communities are designed in [15]. These methods are based on coordinated valley-filling of the load curve via only EV charging and coordinated valley-filling and peak-shaving of the load curve via both EV charging and discharging, respectively; but the renewable energy resources are not considered in [15]. Two methods for optimizing electric vehicle charging in an aggregation of consumers with the objectives of load profile leveling and total cost minimization are proposed in [16]. A two-layer distributed optimization platform with the alternating direction method of multipliers in [17] enhances the load profile's smoothness compared to the locally coordinated and uncoordinated charging platforms. An optimal electric vehicle recharging strategy using quadratic programming for the peak power demand flattening is proposed in [18]. The main drawback of the management systems designed in [11-18] is that they do not fulfill the vehicle requirements.

A penalty factor-based objective function is proposed in [19] for scheduling electric vehicles' coordinated charging and discharging strategy to flatten the daily load curve. A charging management method is proposed in [20] to minimize the total cost and smooth the demand curve with a stochastic distribution function for arrival and departure times. However, renewable energy resources are not considered in [19, 20].

The contributions of this paper are:

1. The demand of vehicle owners has been considered by using four parameters including, arrival time, departure time, initial SoC, and final SoC which are selected randomly without any limit on their values.
2. Some homes have small wind turbines, some homes have photovoltaics, and other homes are without renewable energy sources.
3. A modified mean-field decentralized method is proposed to optimize the charging and discharging of batteries.
4. The vehicle requirements and battery capacity of each vehicle are different.
5. Some vehicles are at home, and the others are in the parking lot.
6. The weighted average method has been modified to increase the accuracy of charging and discharging based on the different capacity of batteries.

In this regard, the remaining of this paper is organized as follows: Section 2 introduces the components of the system, encounters vehicle demands, and proposes a modified mean-field algorithm. Section 3 provides different methods with standard or weighted averaging for every hour or several hours. Section 4 is brought the value of parameters, the value of forecasting output power renewable energies, simulation results, and comparison between different methods. In Section 5, the paper's conclusions are expressed.

## 2. SYSTEM MODELING

In this paper, home customers fall into two categories (Figure 1). The first category only contains loads. In addition to the load, the second category has home-installed renewable energy resources. Renewable energy resources fall into two categories: a photovoltaic and a small wind turbine. Electric vehicle batteries with different battery capacities are also connected to the distribution network, either in the parking lot or home. When a battery is connected to the grid, it declares four parameters: arrival time, departure time, initial SoC, and final SoC. The aggregator smooths the load curve considering the output power of renewable energy resources and the necessary power for the home load and considering the connected batteries declaration and different battery capacities.

Total home power consumption and total production capacity of renewable resources for the customer $n \in N$ at $t \in T$ are considered as $p_n^{D,t}$ and $p_n^{S,t}$, respectively. As a result, the total uncontrollable power for each customer is considered as $p_n^{Un,t} = p_n^{D,t} - p_n^{S,t}$. Production capacity of renewable resources for customer $n \in N$ at $t \in T$ is considered as $p_n^{S,t} = p_n^{PV,t} + p_n^{WT,t}$. The previous days' uncontrollable power curve is used as a power forecast for the next days. Then, the total customer power, including EV battery, is determined as follows:

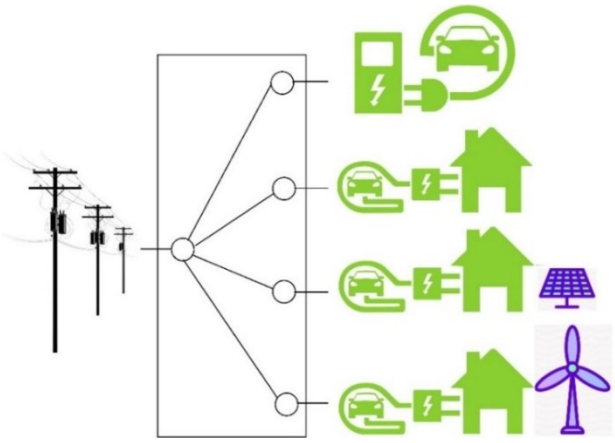

**Fig. 1. Types of connection of electric vehicles to the distribution network**

$$p_n = p_n^{Un} + \gamma_n(q_n^C - q_n^D), \gamma_n = \begin{cases} 1, & t_{arr}^n \le t \le t_{dep}^n \\ 0, & \text{O.W.} \end{cases} \quad (1)$$

where $p_n^{Un} = \left[p_n^{Un,1} \cdots p_n^{Un,T}\right]^T$, $p_n = [p_n^1 \cdots p_n^T]^T$, $q_n^C = \left[q_n^{C,1} \cdots q_n^{C,T}\right]^T$, and $q_n^D = \left[q_n^{D,1} \cdots q_n^{D,T}\right]^T$. $q_n^{C,t}$ and $q_n^{D,t}$ indicate the amount of charge and discharge of the $n^{\text{th}}$ battery at $t \in T$. $t_{arr}^n$ and $t_{dep}^n$ show electric vehicles arrival and departure times, respectively. $\gamma_n$ is defined for the $n^{\text{th}}$ EV according to its arrival and departure times.

The dynamics of SoC is considered as follows [21]:

$$s_n^t = s_n^{t-1} + \frac{\mu_n}{\varsigma_n} q_n^{C,t} - \frac{\mu_n^{-1}}{\varsigma_n} q_n^{D,t}, \quad (2)$$

where:

$0 \le s_n^t \le 1$, $0 \le q_n^{C,t} \le q_n^{C,\max}$, $0 \le q_n^{D,t} \le q_n^{D,\max}$, $s_n^{t_0^n} = SoC_0^n, t_0^n = t_{arr}^n, s_n^{t_F^n} = SoC_F^n, t_F^n = t_{dep}^n$.

$s_n^t$ indicates the SoC of customer $n$ at time $t$ and $SoC_0^n$ and $SoC_F^n$ represent initial and final values of the SoC. $\varsigma_n$ indicates the $n^{\text{th}}$ battery capacity

Note that for $\gamma_n = 0$, the amount of charge and discharge of the battery is assumed to be zero, and the defined optimization problem is solved without considering all the constraints in (2). However, if $\gamma_n = 1$, all constraints in (2) are considered in the optimization problem. Also, due to the different capacities of the batteries, the charging and discharging dynamics of the batteries have different speeds, so these capacities must be taken into account for averaging. The price function is considered as follows:

$$T_n^t(p_n^t, \bar{p}^t) = a_{e,n}^t p_n^t + b_e^t \bar{p}^t + c_e^t, \quad (3)$$

where $a_{e,n}^t \ge 0$ and $b_e^t > 0$, and $\bar{p}$ is defined as:

$$\bar{p} = \sum_{n \in N} \frac{1}{N} p_n, \quad (4)$$

where $\bar{p}$ is $\bar{p} = [\bar{p}^1 \cdots \bar{p}^T]^T$. $a_{e,n}^t$, $b_e^t$, and $c_e^t$ are predetermined parameters. The price function in (3) is effective in moving the load (due to the dependence of the price function on $\bar{p}^t$) and reducing the load (due to the dependence of the price function on $p_n^t$). According to the price function for customer $n$, the daily bill is calculated as follows [21]:

$$E_n^t(p_n^t, \bar{p}^t) = T_n^t(p_n^t, \bar{p}^t) p_n^t, \quad (5)$$

The term $a_{e,n}^t p_n^t$ in (3) converts the electricity bill into a quadratic form, encouraging customers to reduce consumption. The term $b_e^t \bar{p}^t$ also encourages customers not to consume during peak rush hours, and it helps to smooth the load curve. The term $c_e^t$ is for changing electricity tariffs at different times of the day by the distribution network.

The cost of degradation of electric vehicle batteries is considered as follows [21]:

$$H_n(q_n^t) = a_{h,n}\left(\left(q_n^{C,t}\right)^2 + \left(q_n^{D,t}\right)^2\right) + b_h(q_n^{C,t} + q_n^{D,t}), \quad (6)$$

where $q_n^t = \left[q_n^{C,t} \quad q_n^{D,t}\right]^T$. Now, the $n^{\text{th}}$ customer cost function is defined as:

$$U_n(q_n, \bar{p}) = \sum_{t \in T}(E_n^t(p_n^t, \bar{p}^t) + \gamma_n H_n(q_n^t)), \quad (7)$$

where $q_n = [q_n^C \quad q_n^D]^T$. The main task for each customer is to obtain the optimal value of $q_n$ to minimize the cost function in (7). $q_n^C$ and $q_n^D$ are the optimization problem variables which show parameters taken into account during charging and discharging respectively.

According to (7), each customer's strategy affects other customers through $\bar{p}^t$. Also, since each player in the game does not have information about the strategy of other players, this game is not complete. However, since $\bar{p}$ is a common term in the cost function of all players, they do not need to know the optimal strategy of other players. As a result, a modified decentralized mean-field optimization is proposed to solve the problem. In this method, information does not exchange among the players, but is only communicated between the players and the distribution network. That is, the distribution network calculates the optimal strategy for the players and sends the estimated amount of the mean-field term for the next level, to all of them. Thus, the common term $\bar{p}$, called the mean-field term, is estimated by $z(k)$, where $k$ is the step number of the algorithm. By employing $z(k)$ instead of $\bar{p}$, the optimization problem for the $n^{\text{th}}$ player is modified as follows [21]:

$$q_n^*(z(k)) = \underset{q_n}{\operatorname{argmin}}\, U_n(q_n, z(k)), \quad (8)$$

Using the Mann iteration algorithm [22], the update

rule is defined as [21]:

$$z(k+1) = (1-\lambda(k))z(k) + \lambda(k)\Lambda(z(k)) \quad , \quad \Lambda(z(k)) = \sum_{n\in N}\frac{1}{N}p_n^*(z(k)), \quad (9)$$

where $\sum_{k=0}^{\infty}\lambda(k) = \infty$ and $\sum_{k=0}^{\infty}\lambda(k)^2 < \infty$ and for every iteration $k$, $p_n^*\big(z(k)\big) = p_n^{Un} + \gamma_n\left(q_n^{C*}\big(z(k)\big) - q_n^{D*}\big(z(k)\big)\right)$.

The estimation and optimization process is described through the following iterative where each player plans his optimal strategy using the average network consumption. According to the consumption curve of the players in different iterations, estimation of the average network load curve is updated by the distribution network and sent to the players. If customer $n$ cannot send its corresponding $p_n$ value at any iteration, the algorithm continues with the last $p_n$ value sent by the player.

**Modified mean-field algorithm for electric vehicle charging problem:**

initialization

randomly initialize $z(0), k \leftarrow 0$

iteration

for $n \in N$

$q_n^*(z(k)) \leftarrow \underset{q_n}{\operatorname{argmin}}\, U_n(q_n, z(k))$

$p_n^*(z(k)) \leftarrow p_n^{Un} + \gamma_n(q_n^{C*}(z(k)) - q_n^{D*}(z(k)))$

end

$\Lambda\big(z(k)\big) \leftarrow \sum_{n\in N}\frac{1}{N}p_n^*(z(k))$

$z(k+1) \leftarrow (1-\lambda(k))z(k) + \lambda(k)\Lambda(z(k))$

$k \leftarrow k+1$

**Lemma 1:** According to Theorem 3 in [21], if the assumptions of Theorem 2 in [21] are valid and the population of players converges infinitely, then the proposed algorithm converges to the Nash equilibrium point.

## 3. SOLVING THE OPTIMIZATION PROBLEM

Due to the vehicles' information changes and their requests, the calculations shall be updated every hour. On the other hand, due to the different capacities of the batteries, the charging and discharging dynamics of the batteries are different. In the following subsections, five methods are presented to solve the problem.

### 3.1. The first method

In this method, the normal average is used, and due to the change in the number of vehicles and their requests, the calculations of all vehicles are updated per hour.

### 3.2. The second method

In this method, batteries with the same capacity are put in one batch. First, the optimization is done for all vehicles. Then the calculations are updated for the first category in the first hour, the second category in the second hour, and so on. If the number of categories equals $m$, the calculations will be updated in the same way from $m+1$ onwards. Also, the average is done normally per hour.

### 3.3. The third method

In this method, due to the change in the number of vehicles and their requests, the calculations of all vehicles are updated per hour. The weighted average also is used for averaging as follows:

$$\Lambda\big(z(k)\big) = \frac{\alpha_1 p_1^*(z(k)) + \alpha_2 p_2^*(z(k)) + \cdots + \alpha_n p_n^*(z(k))}{\alpha_1+\alpha_2+\cdots+\alpha_n}, \quad (10)$$

in which $\alpha_n = \frac{1}{\varsigma_n}$.

### 3.4. The fourth method

This method is the same as the second method, but the average per hour is calculated using (10).

### 3.5. The fifth method

This method is the same as the second method, but for average, the weighted average is calculated as follows:

$$\Lambda\big(z(k)\big) = \frac{\begin{array}{l}\delta_1\left(p_1^*\left(z(k)\right) + \ldots + p_{r_1}^*\left(z(k)\right)\right) \\ +\delta_2\left(p_{r_1+1}^*\left(z(k)\right) + \ldots + p_{r_2}^*\left(z(k)\right)\right) \\ +\ldots+\delta_v\left(p_{r_{v-1}+1}^*\left(z(k)\right) + \ldots + p_{r_v}^*\left(z(k)\right)\right)\end{array}}{r_1\delta_1 + r_{12}\delta_2 + \ldots + r_{v-1,v}\delta_v}, \quad (11)$$

In (11) $r_{v-1,v} = r_v - r_{v-1}$ and $\delta_n = \frac{1}{\beta_n}$ where $\beta_n$ is computed based on the following simple rule: If $\varsigma_1$ to $\varsigma_{r_1}$ fall into the first category, then $\beta_1 = \frac{\varsigma_1+\varsigma_2+\cdots+\varsigma_{r_1}}{r_1}$. Also, if $\varsigma_{r_1+1}$ to $\varsigma_{r_2}$ fall into the second category, then $\beta_2 = \frac{\varsigma_{r_1+1}+\varsigma_{r_1+2}+\cdots+\varsigma_{r_2}}{r_{12}}$, in which $r_{12} = r_2 - r_1$. The other values of $\beta_i$ are obtained in the same way.

## 4. SIMULATION AND RESULTS

To evaluate the proposed algorithm, a set of 110 customers is considered for sample. The vector $N(t)$ is considered as follows; that the average of $N(t)$ is 110.

$$N = [114\ 103\ 113\ 109\ 114\ 103\ 119\ 103\ 102\ 116\ 119\ 105\ 113\ 101\ 105\ 118\ 115\ 110\ 107\ 104\ 105\ 116\ 108\ 118], \quad (12)$$

20% of customers have a home load, an electric vehicle, and a home-installed photovoltaic. 20% of customers are considered with a home load, an electric vehicle and a home-installed small turbine. 10% of customers have a home load and an electric vehicle. 50% of electric vehicles are also in the parking lot. The load consumption of homes is borrowed from Figure 6

in [23]. The predicted output power of the photovoltaic and wind turbine are also employed in Table 7 of [24]. In this table, the output power is given based on the power of the installed units, as shown in Table 1, and the installed power of photovoltaic and wind turbines in this paper is 1kW. The other parameters are selected as $a_{e,n}^{t} = 1000$, $b_{e}^{t} = 13.5$, $c_{e}^{t} = 0$, $a_{h,n} = 1.2$, $b_{h} = 0$, $\varsigma_{n} = 7.1$, and $\mu_{n} = 0.95$. The battery capacity of each vehicle is randomly selected from the batteries listed in Table 2. The arrival time of all batteries is randomly selected in interval $[1, 10]$. The departure time of all batteries is randomly selected in interval $[13, 24]$. The minimum time between arrival and departure time is 2. There is no limit to choosing between the minimum time of arrival and departure of batteries. However, if the minimum time between arrival and departure time is more than one, the total load curves of this system are very close to each other. The initial SoC of batteries at arrival time is randomly selected in interval $[0, 1]$. The final SoC of batteries at departure time is randomly selected in interval $[0.5, 1]$.

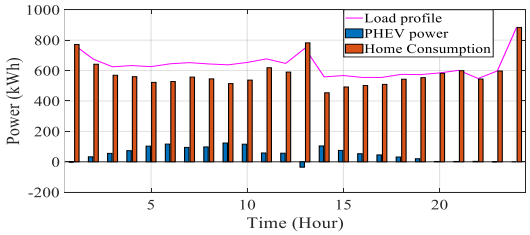


**Fig. 2. Total battery charge, total home load, and total system load curve using method 1**

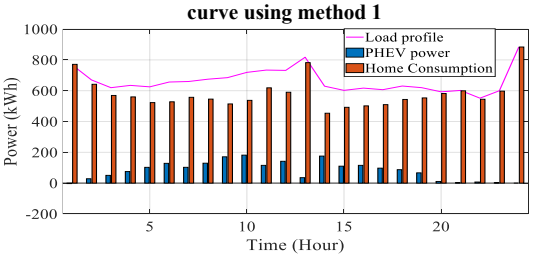


**Fig. 3. Total battery charge, total home load, and total system load curve using method 2**

The number of categories must be a factor of 24, such as 3, 4, 6, or 8. In this paper, 11 types of batteries are considered. Therefore, the number of categories should be 3, 4, or 6. If the number of categories is considered equal to 3 or 6, the capacity of the batteries in each category is very different. As a result, the number of categories should be considered equal to 4 so that the capacity of the batteries in each category is less different and their charging and discharging speeds are very close to each other. The capacity of the first category batteries is less than 25 kWh. The capacity of the second category batteries is in the range of 26 to 35 kWh. The capacity of the third category batteries is in the range of 36 to 45 kWh. The capacity of the fourth category batteries is greater than 46 kWh. Thus, two types of vehicles are in the fourth category, and three types of vehicles are in the first, second, and third categories. The simulation results of this system using five different methods are seen in Figures 2 to 6. Calculations are updated every hour according to the vector $N(t)$. Table 3 compares the different types of problem-solving methods. According to Table 3, the load curve of the first and third methods have the lowest values, but the simulation time of these methods is very long. The variance of the fourth and fifth methods is slightly different from the first method, but the simulation time of these two methods is one-third of the simulation time of the first method.

**Table 1. Output power of photovoltaic and wind turbine**

| Hour | power of photovoltaic (kW) | power of wind turbine (kW) |
|---|---|---|
| 1 | 0 | 0.119 |
| 2 | 0 | 0.119 |
| 3 | 0 | 0.119 |
| 4 | 0 | 0.119 |
| 5 | 0 | 0.119 |
| 6 | 0 | 0.061 |
| 7 | 0 | 0.119 |
| 8 | 0.008 | 0.087 |
| 9 | 0.15 | 0.119 |
| 10 | 0.301 | 0.206 |
| 11 | 0.418 | 0.585 |
| 12 | 0.478 | 0.694 |
| 13 | 0.956 | 0.261 |
| 14 | 0.842 | 0.158 |
| 15 | 0.315 | 0.119 |
| 16 | 0.169 | 0.087 |
| 17 | 0.022 | 0.119 |
| 18 | 0 | 0.119 |
| 19 | 0 | 0.0868 |
| 20 | 0 | 0.119 |
| 21 | 0 | 0.0867 |
| 22 | 0 | 0.0867 |
| 23 | 0 | 0.061 |
| 24 | 0 | 0.041 |

**Table 2. Types of vehicles and battery capacity of each vehicle [25]**

| Brand | Model | Battery capacity (kWh) | $q_{n}^{C,\max}$, $q_{n}^{D,\max}$ |
|---|---|---|---|
| Chevrolet | Spark EV | 18.3 | 7.32 |
| Honda | FIT | 20 | 8 |
| Fiat | 500e | 24 | 9.6 |
| BMW | i3 | 27.2 | 10.88 |
| Mercedes | B250e | 28 | 11.2 |
| Ford | Focus-e | 33.5 | 13.4 |
| Hyundai | Ioniq-e | 38.3 | 15.32 |
| Nissan | LEAF | 40 | 16 |
| Toyota | RAV4 | 41.8 | 16.72 |
| Kia | Soul EV | 64 | 25.6 |
| Tesla | Model 3 | 78 | 31.2 |

The most accurate method of energy management is the third method. Because the calculations are updated, every hour and the weighted average is used. Among the second, fourth, and fifth methods, the lowest time and the lowest variance belong to the fifth method. As a result, the fifth method has the most negligible difference inaccuracy from the third method and the

lowest computational cost related to other methods.

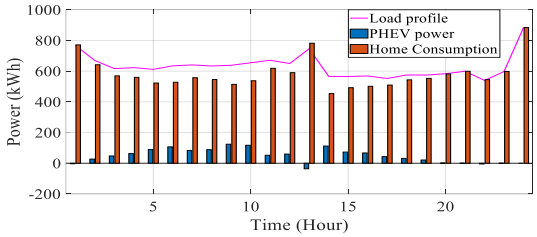


**Fig. 4. Total battery charge, total home load, and total system load curve using method 3**

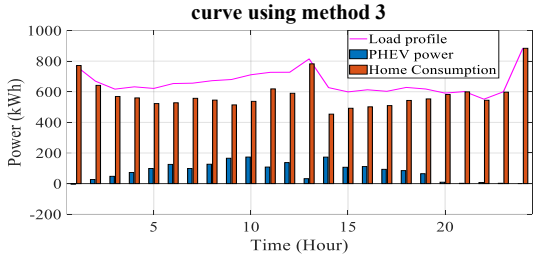


**Fig. 5. Total battery charge, total home load, and total system load curve using method 4**

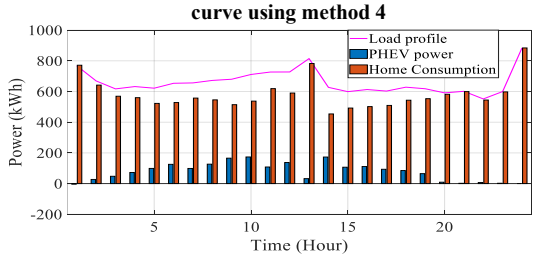


**Fig. 6. Total battery charge, total home load, and total system load curve using method 5**

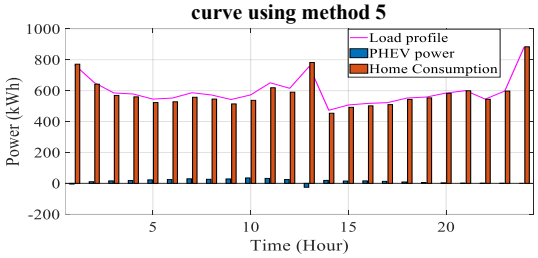


**Fig. 7. Total battery charge, total home load, and total system load curve using method 6 (Eq. (14))**

Differences between the load profiles in five methods were quantified in Table 4. This table lists the sum of absolute values of the differences. According to Table 4, method five has differed the accuracy of calculation for mean load values per day by 0.0410 compared to method four. This value is for all vehicles for 24 hours. As a result, given that this value is minimal, methods four and five are very similar. According to Table 4, method five has deteriorated the calculation accuracy for mean load values per day by 702.7227 compared to exact method three. When this value is divided by 24 (number of hours), the accuracy of the calculations of all vehicles per hour is reduced by $702.7227/24 = 29.2801$. When this value is divided by 110 (number of vehicles), the accuracy of the calculations of each vehicle per hour is reduced by $29.2801/110 = 0.2661$, and this value is small. Now, for further comparison, the cost function suggested in [26], [27] and [28] is used to smooth the load curve as follows:

**Table 3. A comparison between different types of problem solving methods**

| Type of method | Simulation time (mins) | Load curve variance | Load curve average |
|---|---|---|---|
| Method 1 | 425.6588 | 6101.4644 | 634.5865 |
| Method 2 | 144.3774 | 6069.7710 | 663.7968 |
| Method 3 | 412.0885 | 6016.5883 | 631.7689 |
| Method 4 | 122.9922 | 6027.3486 | 661.0485 |
| Method 5 | 122.7103 | 6027.2927 | 661.0472 |

**Table 4. Absolute mean value summation of a day load profile differences between vertical and horizontal methods.**

| MSAD (kW) | Method 1 | Method 2 | Method 3 | Method 4 | Method 5 |
|---|---|---|---|---|---|
| Method 1 | 0 | 699.2710 | 69.3976 | 640.6499 | 640.6195 |
| Method 2 | 699.2710 | 0 | 768.6686 | 65.9582 | 65.9912 |
| Method 3 | 69.3976 | 768.6686 | 0 | 702.7560 | 702.7227 |
| Method 4 | 640.6499 | 65.9582 | 702.7560 | 0 | 0.0410 |
| Method 5 | 640.6195 | 65.9912 | 702.7227 | 0.0410 | 0 |

**Table 5. Load curve values of different methods.**

| Hour | Method 1 | Method 2 | Method 3 | Method 4 | Method 5 | Method 6 |
|---|---|---|---|---|---|---|
| 1 | 769.5493 | 768.0633 | 768.8265 | 767.8265 | 767.8268 | 766.7869 |
| 2 | 674.6690 | 669.9799 | 669.0082 | 668.9853 | 668.9855 | 652.1458 |
| 3 | 624.8781 | 619.6607 | 616.8008 | 617.0764 | 617.0746 | 585.1712 |
| 4 | 632.9860 | 634.5849 | 622.9583 | 632.1850 | 632.1833 | 578.1284 |
| 5 | 625.9126 | 625.0948 | 611.5435 | 621.6684 | 621.6673 | 545.1626 |
| 6 | 644.6734 | 656.3721 | 634.6844 | 653.5745 | 653.5738 | 552.1071 |
| 7 | 652.1602 | 659.8319 | 640.6262 | 656.0485 | 656.0479 | 586.5229 |
| 8 | 643.5990 | 674.8653 | 633.7933 | 672.2098 | 672.2096 | 571.9212 |
| 9 | 637.8277 | 684.8080 | 638.2357 | 679.9228 | 679.9208 | 542.6272 |
| 10 | 653.4581 | 719.1460 | 654.7879 | 710.9893 | 710.9824 | 572.4726 |
| 11 | 676.8785 | 734.0201 | 670.8548 | 726.9190 | 726.9135 | 650.8033 |
| 12 | 647.0647 | 731.9233 | 649.9110 | 727.3953 | 727.3909 | 615.1933 |
| 13 | 746.7181 | 817.4244 | 746.0042 | 814.4858 | 814.4849 | 756.8301 |
| 14 | 558.3422 | 629.3607 | 565.9970 | 627.0224 | 627.0200 | 473.0411 |
| 15 | 567.3910 | 602.2662 | 565.2135 | 599.1415 | 599.1397 | 507.2979 |
| 16 | 554.8226 | 616.8894 | 568.6948 | 612.8758 | 612.8736 | 517.3769 |
| 17 | 554.9932 | 606.6572 | 552.3988 | 602.8538 | 602.8505 | 522.3959 |
| 18 | 575.1415 | 630.4439 | 575.0279 | 628.2429 | 628.2415 | 552.1549 |
| 19 | 573.3790 | 619.7551 | 574.4317 | 618.0139 | 618.0150 | 558.6888 |
| 20 | 584.6023 | 592.7753 | 583.3017 | 591.1796 | 591.1808 | 584.5381 |
| 21 | 601.7973 | 601.9284 | 599.3462 | 601.2863 | 601.2877 | 600.0940 |
| 22 | 547.8465 | 551.5660 | 539.6317 | 551.5561 | 551.5562 | 544.9662 |
| 23 | 597.4385 | 599.7598 | 597.4298 | 599.7592 | 599.7592 | 597.4062 |
| 24 | 883.9468 | 883.9468 | 883.9468 | 883.9468 | 883.9468 | 883.9468 |

$$\Delta P_t = \left|\sum_{i=1}^{N(t)} p_i^{D,t} - \sum_{i=1}^{N(t)} p_i^{PV,t} - \sum_{i=1}^{N(t)} p_i^{WT,t} + \gamma_n\left(\sum_{i=1}^{N(t)} q_i^{C,t} - \sum_{i=1}^{N(t)} q_i^{D,t}\right) - p_{grid}^{spec}\right| \quad (13)$$

where $p_{grid}^{spec}$ is the specified grid power and is considered as the average of the load curve. Equation (13) is used to smooth the load curve per hour $t$. The cost function for time interval $t$ is obtained by adding the battery degradation cost (6) to (13) as follows:

$$C = \Delta P_t + \gamma_n H_n(q_n^t), \quad (14)$$

In Figure 7, the simulation result of the system using (14) is seen with the same parameters as the other methods. Also, $p_{grid}^{spec}$ is equal to the average of methods 4 and 5 ($p_{grid}^{spec} = 661$). In this method, load curve variance and load curve average are equal to 8440.8167 and 596.5741, respectively. The variance of methods 4 and 5 is much less than method 6, and these methods help to smooth the load

curve much more. Also, the load curve values of Figures 2-7 are given in Table 5.

## 5. CONCLUSIONS

Various problem-solving methods for smoothing the load curve were examined with different types of connections of electric vehicle batteries in homes and parking lots. The output power of home-installed small wind turbines and photovoltaics using the forecast based on previous days' information was applied in the optimization. The proposed algorithm satisfies the demands of vehicles well, and smoothes the load curve efficiently. Therefore, by using this algorithm and meeting customer needs, the profit of both the distribution network and the customers is maximized. In this regard, instead of using the normal average, the weighted average is used for power management, and the calculations for each vehicle are updated every four hours. The variance of the proposed method is less than one percent different from the most accurate method, but the computational cost of the method is 3.5 times lower. The calculation time of methods 4 and 5 is 3.3 times shorter than method 3 (the most accurate method).

## REFERENCES


[1] H. Shayeghi and E. Shahryari, "Optimal operation management of grid-connected micro-grid using multi-objective group search optimization algorithm", *J. Oper. Autom. Power Eng.*, vol. 5, no. 2, pp. 227-239, 2017.

[2] J. Guerrero et al., "Towards a transactive energy system for integration of distributed energy resources: Home energy management, distributed optimal power flow, and peer-to-peer energy trading", *Renew. Sustain. Energy Rev.*, vol. 132, 2020.

[3] M. Belgacem, B. Gassara, and A. Fakhfakh, "Design and implementation of multi-source and multi-consumer energy sharing system in collaborative smart micro-grid installation", *J. Oper. Autom. Power Eng.*, vol. 10, no. 3, pp. 189-199, 2022.

[4] S. Chupradit et al., "Modeling and optimizing the charge of electric vehicles with genetic algorithm in the presence of renewable energy sources", *J. Oper. Autom. Power Eng.*, 2022.

[5] A. Geetha and C. Subramani, "A comprehensive review on energy management strategies of hybrid energy storage system for electric vehicles", *Int. J. Energy Res.*, vol. 41, no. 13, pp. 1817-1834, 2017.

[6] T. Logenthiran, D. Srinivasan, and T. Shun, "Demand side management in smart grid using heuristic optimization", *IEEE Trans. Smart Grid*, vol. 3, no. 3, pp. 1244-1252, 2012.

[7] M. Jarnut, S. Wermiński, and B. Waśkowicz, "Comparative analysis of selected energy storage technologies for prosumer-owned micro-grids", *Renew. Sustain. Energy Rev.*, vol. 74, pp. 925-937, 2017.

[8] S. Ayyadi, H. Bilil, and M. Maaroufi, "Optimal charging of electric vehicles in residential area", *Sustain. Energy, Grids Net.*, vol. 19, 2019.

[9] E. Reihani et al., "Energy management at the distribution grid using a battery energy Storage system (BESS)", *Int. J. Electr. Power Energy Syst.*, vol. 77, pp. 337-344, 2016.

[10] E. Reihani et al., "Load peak shaving and power smoothing of a distribution grid with high renewable energy penetration", *Renew. Energy*, vol. 86, pp. 1372-1379, 2016.

[11] R. Sebastián, "Application of a battery energy storage for frequency regulation and peak shaving in a wind diesel power system", *IET Gener. Transm. Distrib.*, vol. 10, no. 3, pp. 764-770, 2016.

[12] S. Chapaloglou et al., "Smart energy management algorithm for load smoothing and peak shaving based on load forecasting of an island's power system", *Appl. Energy*, vol. 238, pp. 627-642, 2019.

[13] N. Attou et al., "Improved peak shaving and valley filling using V2G technology in grid connected microgrid", *Third Int. Conf. Transport. Smart Tech.*, pp. 53-58, 2021.

[14] M. Hashim et al., "Priority-based vehicle-to-grid scheduling for minimization of power grid load variance", *J. Energy Storage*, vol. 39, 102607, 2021.

[15] N. Nimalsiri et al., "Coordinated charge and discharge scheduling of electric vehicles for load curve shaping", *IEEE Trans. Intell. Transport. Syst.*, pp. 1-13, 2021.

[16] F. Palmiotto et al., "A coordinated optimal programming scheme for an electric vehicle fleet in the residential sector", *Sustain. Energy Grids Net.*, vol. 28, 2021.

[17] S. Afshar et al., "A distributed electric vehicle charging scheduling platform considering aggregators coordination", *IEEE Access*, vol. 9, pp. 151294-05, 2021.

[18] C. Padhi, S. Panda, and G. Biswal, "Optimal recharging of EVs for peak power shaving and valley filling using EV-aggregator model in a micro-grid", *J. Physics: Conf. Series*, vol. 1854, no. 1, 2021.

[19] S. Das et al., "Optimal management of vehicle-to-grid and grid-to-vehicle strategies for load profile improvement in distribution system", *J. Energy Storage*, vol. 49, 2022.

[20] A. Hasankhani et al., "Day-ahead optimal management of plug-in hybrid electric vehicles in smart homes considering uncertainties", *IEEE PowerTech*, 2021.

[21] M. Shokri, and H. Kebriaei, "Mean-field optimal energy management of plug-in hybrid electric vehicles", *IEEE Trans. Veh. Tech.*, vol. 68, no. 1, pp. 113-120, 2018.

[22] V. Berinde and F. Takens, Iterative approximation of fixed points, vol. 1912, Berlin: Springer, 2007.

[23] A. Safdarian et al., "Distribution network reliability improvements in presence of demand response", *IET Gener. Transm. Distrib.*, vol. 8, pp. 2027-35, 2014.

[24] A. Moghaddam et al., "Multi-objective operation management of a renewable MG (micro-grid) with back-up micro-turbine/fuel cell/battery hybrid power source", *Energy*, vol. 36, no. 11, pp. 6490-6507, 2011.

[25] Y. Jin et al., "Optimal aggregation design for massive V2G participation in energy market", *IEEE Access*, vol. 8, 211794-808, 2020.

[26] K. Reddy and S. Meikandasivam, "Load flattening and voltage regulation using plug-in electric vehicle's storage capacity with vehicle prioritization using anfis", *IEEE Trans. Sustain. Energy*, vol. 11, pp. 260-270, 2018.

[27] K. Reddy, S. Meikandasivam, and D. Vijayakumar, "A novel strategy for maximization of plug-in electric vehicle's storage utilization for grid support with consideration of customer flexibility", *Electr. Power Syst. Res.*, vol. 170, pp. 158-175, 2019.

[28] S. Meikandasivam, "Optimal distribution of plug-in-electric vehicle's storage capacity using water filling algorithm for load flattening and vehicle prioritization using ANFIS", *Electr. Power Syst. Res.*, vol. 165, pp. 120-133, 2018.